Visible and infrared transparency in lead-free bulk $BaTiO_3$ and $SrTiO_3$ nanoceramics

2010 Nanotechnology 21 075706

(http://iopscience.iop.org/0957-4484/21/7/075706)

Nanotechnology **21** (2010) 075706 (5pp) doi:10.1088/0957-4484/21/7/075706

Visible and infrared transparency in lead-free bulk $BaTiO_3$ and $SrTiO_3$ nanoceramics

Jing Liu[1,2], Zhijian Shen[1], Wenlong Yao[2], Yonghao Zhao[2] and Amiya K Mukherjee[2]

[1] Department of Physical, Inorganic and Structural Chemistry, Arrhenius Laboratory, Stockholm University, S-106 91 Stockholm, Sweden
[2] Department of Chemical Engineering and Materials Science, University of California, Davis, CA 95616, USA

E-mail: jwliu@ucdavis.edu

Received 24 September 2009, in final form 21 December 2009
Published 18 January 2010
Online at stacks.iop.org/Nano/21/075706

Abstract
Multifunctional transparent ferroelectric ceramics have widespread applications in electro-optical devices. Unfortunately, almost all currently used electro-optical ceramics contain a high lead concentration. In this work, via coupling of spark plasma sintering with high pressure, we have successfully synthesized bulk lead-free transparent nanostructured $BaTiO_3$ (abbreviated as BTO) and $SrTiO_3$ (STO) ceramics with excellent optical transparency in both visible and infrared wavelength ranges. This success highlights potential ingenious avenues to search for lead-free electro-optical ceramics.

1. Introduction

Polycrystalline transparent ferroelectric ceramics have been attracting a great deal of attention because of their unique combination of optical and ferroelectric properties [1, 2], and their low production cost compared with conventional single crystalline ferroelectric materials, such as $LiNbO_3$ [3] and $(Sr, Ba)Nb_2O_6$ [4]. Multifunctional transparent ferroelectric ceramics can be used as electro-optical devices including optical modulation devices, optical shutters and switchers, as well as image memory devices [5, 6]. However, almost all well-developed electro-optical ceramics, such as $(Pb, La)(Zr, Ti)O_3$ [PLZT], contain lead [1, 5]. These lead-containing electro-optical ceramics are not only harmful to the environment [7], but can also gradually degrade their optical efficacy due to volatilization of lead [6]. There has been a continuous search for lead-free green optical transparent ferroelectric ceramics, but with no clear evidence of success on record.

Optical transparency is the key towards multifunctional polycrystalline electro-optical ceramics. A review of the published literature suggests that porosity (density) and grain size are the two most critical structural parameters determining the transparency of ceramics [5, 8–12]. Extremely high density (low porosity) is necessary for transparency due to the high efficiency of pores as light scattering regions. With those ceramics having larger grain size (>5 μm) it is difficult to fully avoid the existence of big pores (>20 nm). Recent investigations suggest that nanometric grain size is favorable to optical transparency [11]. However, it is still a challenge to synthesize bulk nanostructured transparent ceramics since the density and grain size are traded-off each other under traditional sintering techniques. That is, the high density can be achieved under sintering conditions involving high temperatures and long hold times which sacrifice the nanostructures and vice versa. Therefore, most nanostructured transparent ceramics were applied as thin films [13, 14]. However, ceramic thin films are at a disadvantage in comparison to bulk ceramics for structural applications because of poor mechanical properties such as hardness and durability.

In this work, as described in detail below, we used a relatively new rapid sintering technique—high-pressure spark plasma sintering (SPS) [12]—to prepare bulk optical transparent nanostructured BTO and STO nanoceramics. The high pressure and short sintering time impede grain growth while densifying the sample. The BTO and STO ceramics were selected as they are the most well-investigated lead-free

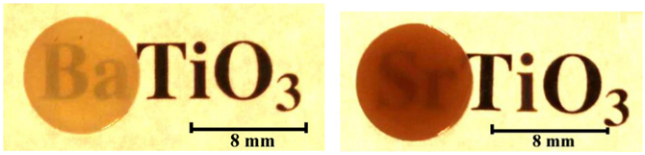

Figure 1. Sample photos of the transparent/translucent BTO (a) and STO (b) ceramics.

ABO_3 perovskite materials [15, 16]. In the literature, bulk polycrystalline STO and BTO are optically opaque, except in their single crystalline state [17, 18] and occasionally in thin films [19, 20], which have been demonstrated to exhibit optical transmissions. This success highlights potential ingenious avenues to search for new lead-free electro-optical ceramics.

2. Experimental details

Commercially available monophasic nano-$BaTiO_3$ and $SrTiO_3$ powders with particle sizes of 60–80 nm (TPL Inc., Albuquerque, NM, USA) were used as starting sintering powders. The SPS sintering process was performed at Dr Sinter 2050 (Sumitomo Coal Mining Co. Ltd, Japan). Bulk BTO and STO disks (⌀8 × 2 mm) were sintered in vacuum under a uniaxial pressure of 200 MPa at 900 or 950 °C holding for 3 min with a heating rate of 100 °C min^{-1}. Dual wall graphite dies were used in the SPS process to reach high pressures. The high pressure was applied when reaching the preset temperature during the SPS process. The temperature was regulated by a thermocouple that was inserted into the outer wall of the graphite die. The sintered samples were post-SPS annealed at 750 °C for 200 min in air in order to ensure full oxidation and remove all traces of carbon. The heating rate of the post-SPS annealing process was around 10 °C min^{-1}, and then it cooled down to room temperature at a cooling rate of approximately 8 °C min^{-1} to release the residual stress.

The optical visible and infrared transmissions were measured by an ultraviolet and visible spectrometer (UV–vis Perkin Lambda 19) and Bruker IFS 66v/s spectrometer, respectively. The optical-measurement samples were well polished by using a series of diamond pastes and gamma Al_2O_3 powder with a particle size of 50 nm to the dimension of parallel plates with a thickness of 0.8–0.9 mm. A silver paste electrode was fabricated on the surface of the ceramic samples. A Hewlett-Packard 4192 LF impedance analyzer was used to determine the dielectric properties using frequencies ranging from 10^2 to 10^7 Hz. The experimental set-up consisted of an He-flow cryostat allowing the measurement of temperatures down to 5 K. Micrographs of the fracture surfaces were recorded in a scanning electron microscope (SEM; JSM-7401F, JEOL, Tokyo, Japan). The bulk densities were measured according to Archimedes' principle.

3. Results and discussion

We consolidated BTO and STO nano-powders within their sintering temperature 'kinetic window' [21] by SPS at high pressure (200 MPa). Bulk transparent ceramics with a dimension of ⌀8 × 2 mm were successfully achieved at sintering temperatures of 900 °C for BTO and 950 °C for STO. Their densities were measured as 5.97 g cm^{-3} (99.2% theoretical density TD) and 5.08 g cm^{-3} (99.3% TD), respectively. Sample photos, as displayed in figure 1, clearly show the visible transparencies/translucencies of ceramics.

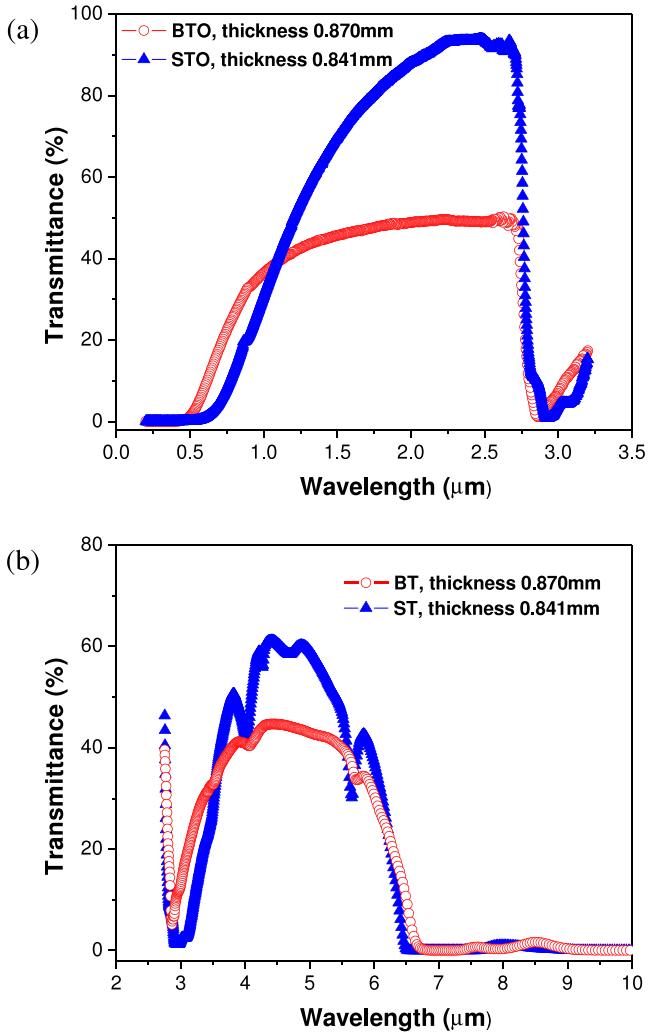

Figure 2. Transmission spectra of nanostructured BTO and STO ceramics in (a) the UV–vis–NIR wavelength range and (b) the IR wavelength range. The thicknesses of the specimen are 0.870 mm for BTO and 0.841 mm for STO, respectively.

To measure the optical properties, both BTO and STO ceramics were well polished to have parallel plate surfaces with thicknesses of 0.870 mm and 0.841 mm, respectively. Figure 2(a) displays the UV–visible–near IR (UV–vis–NIR) transmission spectra of BTO and STO ceramics. Within the measured wavelength, both BTO and STO ceramics have broad transmission spectra starting from about 450 (for BTO) and 560 nm (for STO), respectively, while ending at a similar wavelength at the near IR region (2.9 μm). The nanostructured STO ceramic showed super vis–NIR transmittance (around 90%) and the nanostructured BTO ceramic still has a very good vis–NIR transmittance (around 50%). The super vis–NIR transmittance observed in STO is, at least, comparable with the

value of an STO single crystal (85–90%) [17, 18]. It should be pointed out that, to the best of our knowledge, no transparent STO ceramics in the visible spectrum have been reported in the literature, although great efforts have been made during the last two decades [21–23].

Figure 2(b) shows the infrared (IR) transmission spectra of the nanostructured BTO and STO ceramics. Similar to the UV–vis–NIR results, BTO has a slightly broader and much lower IR transmission spectrum (starting from 2.9 μm and ending at 6.7 μm) than the STO (starting from 2.9 μm and ending at 6.5 μm). The transmittances in both samples reach maxima in the wavelength range of 4.2–5 μm. Compared with the IR transmission spectra of single crystal STO [17, 18], both of the BTO and STO ceramics exhibit a strong absorption peak at around 2.9 μm. This absorption peak for both BTO and STO ceramics might be generated from –OH stretching vibration [24]. A certain amount of water is assumed to be trapped within the sintered samples due to the strong absorption of water in the original BTO and STO nano-powders and the fast heating process during SPS sintering. In addition, we detected another absorption peak at around 5.6 μm in the IR transmission spectra of the BTO and STO ceramics. This peak corresponds to the TiO_2 absorption peak [23].

For the multifunctional electro-optical BTO and STO, ferroelectric properties are also important along with the optical properties discussed earlier. Figure 3 shows the temperature dependence of the permittivity ε_r and dielectric loss tan(δ) at 100 kHz for both BTO and STO ceramics. Compared to micro-structured BTO ceramics reported in the literature [16, 25, 26], the nanostructured BTO ceramic shows relatively low and less temperature-dependent ε_r and tan(δ) within the measured temperature range (from 293 to 453 K), suggesting a very broad phase transition. $BaTiO_3$ ceramics are well known for their remarkable dielectric properties and their permittivity depends strongly on the grain size [25, 26]. The micro-structured BTO ceramics show a temperature-dependent ε_r and the ε_r values are generally larger than 4000 in the vicinity of its Curie temperature, T_C (127 °C) [15, 26, 27]. Similar to the BTO, the ε_r and tan(δ) of the nanostructured STO ceramic is dramatically low, particularly at low temperatures (<50 K), in comparison with micro-structured STO ceramics [22, 23]. The decrease of ε_r in the nanostructured BTO and STO ceramics is mainly due to their small grain sizes [22, 26]. The amount of the polar dead layer at grain boundaries, possessing a smaller permittivity, increases significantly with reducing grain size down to the nanometer region [22, 26]. The intrinsic size effect may also have an influence on the depression of the permittivity of nanostructured BTO and STO ceramics. The soft mode disappears below the critical grain size (a number of unit cells), and the mechanism of ferroelectric phase transition changes [26, 28]. The present dielectric properties of the nanostructured BTO and STO ceramics concur with previous studies [21, 22].

To uncover the underlying mechanisms for the above electro-optical properties of BTO and STO samples, we analyzed micro-structures by scanning electron microscopy

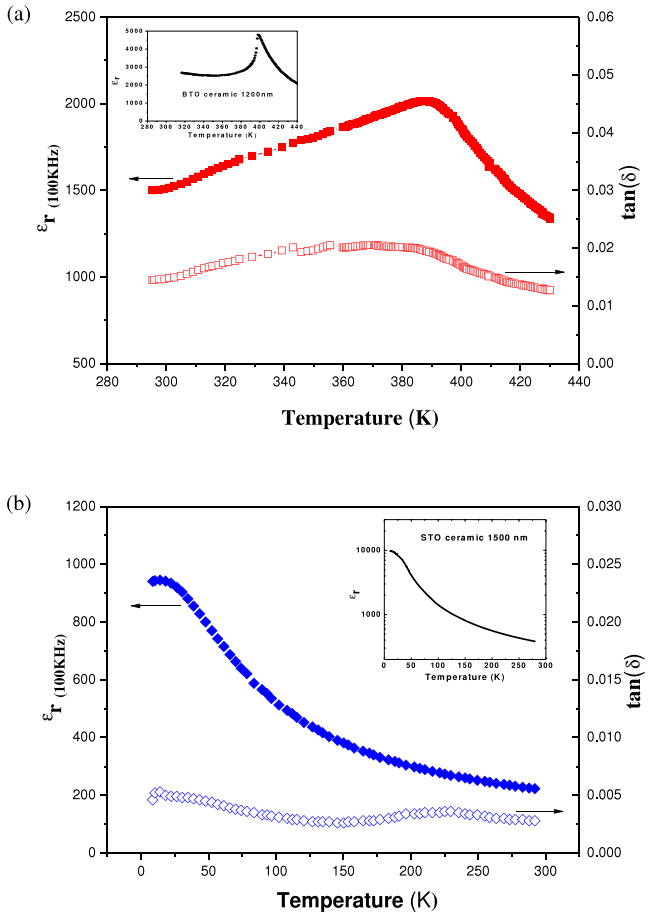

Figure 3. Temperature dependence of permittivity (ε_r) and dielectric loss tan(δ) at 100 kHz of the (a) BTO and (b) STO ceramics. Micro-structured BTO and STO ceramics data from literature [27, 19] were inserted to compare with our data. (This figure is in colour only in the electronic version)

(SEM) and x-ray diffraction (XRD). The fracture surfaces of BTO and STO samples, imaged by SEM, are shown in figure 4. It is apparent that the fracture surfaces of both BTO and STO samples are composed of uniform nanometric grains. The majority of the grains in STO have sizes smaller than 100 nm, while most grains in BTO are larger than 100 nm. Moreover, from figure 4, both BTO and STO ceramics are highly dense due to the fact that very few residual open pores can be discerned; if any, they are of a diameter smaller than 20 nm or so. XRD measurements reveal that BTO and STO have, respectively, tetragonal and cubic crystalline structures at room temperature. This agrees with our previous investigations [21].

As discussed in section 1, density (pores) and grain size are two critical parameters determining transparency of ceramics. The transparency in the nanostructured STO and BTO is a result of both high density (higher than 99.2% of their TD) and smaller grains (less than 200 nm). General visible-spectrum light corresponds to a wavelength range of 380–780 nm. To ensure transparencies of ceramics, the grain sizes should evade this range, i.e. either smaller than 380 nm [12, 24] or much larger than 780 nm [9]. Moreover, a decrease in grain size concurrently reduces the pore size, and the latter

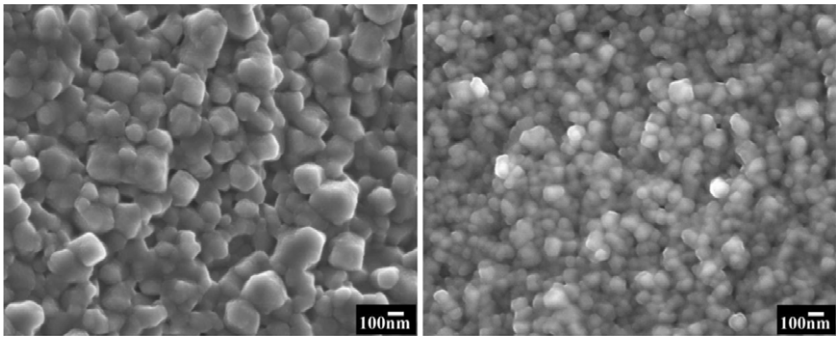

Figure 4. SEM micrographs of the nanostructured BTO (a) and STO (b) samples.

is expected to have significant influence on transparency. The residual pores for both BTO and STO ceramics are smaller than 20 nm or so in diameter through SEM images. Those residual open pores are too small to scatter light [19]. This explains why the nanostructured ceramics provide better transparency than micro-structured ceramics [12]. The grain size effect is more pronounced for a shorter wavelength. This may be the reason why the nanostructured STO ceramic has a relatively high short-wavelength cut-off in comparison to the corresponding single crystal data of STO [17, 18].

As compared with BTO, STO has a better transmittance. This can be attributed to the following factors. First, the grain size of STO is smaller than BTO and, as mentioned above, smaller grain size is beneficial to optical transparency. Second, at room temperature STO has a cubic crystal structure, which exhibits better optical transmission spectra than BTO the structure of which is of tetragonal symmetry. When the light passes through grain boundaries from a grain to its neighboring grain, it is refracted and reflected (scattered) at each grain boundary for non-cubic crystal structure [24], while no refraction or reflection (optical scatter) occurs in the case of a cubic system.

4. Conclusions

In summary, employing high pressure SPS, we produced lead-free green bulk-dense nanostructured BTO and STO transparent ceramics. Both BTO and STO ceramics showed excellent optical properties in both vis–NIR and IR wavelength ranges and relatively low, and almost temperature independent, permittivity and dielectric loss. The optical transmittance in nanostructured STO ceramic is comparable to that of STO single crystal data. Our work demonstrates a promising method to synthesize multifunctional lead-free electro-optical ceramics with important applications in electro-optical devices.

Acknowledgments

This work was sponsored by the Swedish Research Council and the US Office of Naval Research.

References

[1] Haertling G H and Land C E 1971 *J. Am. Ceram. Soc.* **54** 1–11
[2] Wu Y J and Li J 2005 *J. Am. Ceram. Soc.* **88** 3327–31
[3] Bergman J G, Ashkin A, Ballman A A, Dziedzic J M, Levinstein H J and Smith R G 1968 *Appl. Phys. Lett.* **12** 92–4
[4] Ewbank M D, Neurgaonkar R R, Cory W K and Feinberg J 1987 *J. Appl. Phys.* **62** 374–80
[5] Silva D D and Boccaccini A R 2008 *Recent Patents on Mater. Sci.* **1** 56–73
[6] Li K K and Wang Q 2003 Electro-optic lead barium lanthanum zinc niobate titanate ceramics for optical communication devices with low propagation loss *US Patent Specification* (Corning Inc., USA) p 16
[7] Setter N 2002 Piezoelectric materials and devices *Piezoelectric Materials and Devices* (Lausanne, Switzerland: Swiss Federal Institute of Technology)
[8] Peelen J G J and Metselaar R 1974 *J. Appl. Phys.* **45** 216–20
[9] Apetz R and van Bruggen M P B 2003 *J. Am. Ceram. Soc.* **86** 480–6
[10] Jain M, Skandan G, Singhal A, Agrawal D, Feng Y, La Monica J and Kirsch J 2005 *Proc. SPIE-Int. Soc. Opt. Eng.* **5786** 217–26
[11] Stefanik T, Gentilman R and Hogan P 2007 *Proc. SPIE-Int. Soc. Opt. Eng.* **6545** 65450
[12] Anselmi-Tamburini U, Woolman J N and Munir Z A 2007 *Adv. Funct. Mater.* **17** 3267–73
[13] Liang Y-C and Liang Y-C 2009 *Scr. Mater.* **61** 117–20
[14] Jellison G E Jr, Boatner L A, Lowndes D H, McKee R A and Godbole M 1994 *Appl. Opt.* **33** 6053–8
[15] Haertling G H 1999 *J. Am. Ceram. Soc.* **82** 797–818
[16] Takeuchi T, Tabuchi M, Kageyama H and Suyama Y 1999 *J. Am. Ceram. Soc.* **82** 939–43
[17] Linsteadt G 1964 *Appl. Opt.* **3** 1453–6
[18] Popovic D, Romcevic N, Spasovic S, Dojcilovic J, Golubovic A and Nikolic S 2006 *J. Alloys Compounds* **425** 50–3
[19] Shimooka H, Kohiki S, Kobayashi T and Kuwabara M 2000 *J. Mater. Chem.* **10** 1511–2
[20] Cho J-H, Choi W-Y, Kim S-H and Kuwabara M 2005 *Integr. Ferroelectr.* **69** 287–93
[21] Liu J, Shen Z, Nygren M, Su B and Button T W 2006 *J. Am. Ceram. Soc.* **89** 2689–94
[22] Petzelt J, Ostapchuk T, Gregora I, Kuzel P, Liu J and Shen Z 2007 *J. Phys.: Condens. Matter* **19** 196222
[23] Petzelt J, Ostapchuk T, Gregora I, Savinov M, Chvostova D, Liu J and Shen Z 2006 *J. Eur. Ceram. Soc.* **26** 2855–9

[24] Harris D C 1999 *Materials for Infrared Windows and Domes: Properties and Performance* (Washington, DC: SPIE-The International Society for Optical Engineering)
[25] Arlt G, Hennings D and De With G 1985 *J. Appl. Phys.* **58** 1619–25
[26] Zhao Z, Buscaglia V, Viviani M, Buscaglia M T, Mitoseriu L, Testino A, Nygren M, Johnsson M and Nanni P 2004 *Phys. Rev.* B **70** 024107
[27] West A R, Adams T B, Morrison F D and Sinclair D C 2004 *J. Eur. Ceram. Soc.* **24** 1439–48
[28] Fridkin V M 2004 *J. Phys.: Condens. Matter* **16** 7599–602